

Entry Trajectory Optimization via hp Pseudospectral Convex Programming

Xiao Wang^a, Yulin Wang^b, Shengjing Tang^c and Jie Guo^d
School of Aerospace and Engineering, Beijing Institute of Technology, Beijing, China

Keywords: Entry Guidance, Trajectory Optimization, Convex Programming, Pseudospectral Method.

Abstract: In this paper, a hp pseudospectral sequential convex programming (hp-PSCP) method is proposed to solve the entry trajectory optimization problem. The hp flipped Radau pseudospectral method (FRPM) is utilized to discretize the nonlinear dynamics. By successive linearization technology and introducing new variables, the optimization problem is converted into a series of convex problems and solved by primal-dual interior-point method. Numerical results show that the proposed method provides a good compromise between computational accuracy and speed compared to existing convex methods.

1 INTRODUCTION

Entry phase, which is from space to atmosphere, is the key stage for the flight of entry vehicles, including reusable launch vehicles and hypersonic gliding vehicles. Entry guidance is always a difficult issue of the research of entry vehicles (Lu, 2014). With the development of onboard entry guidance, requirements for online trajectory optimization methods are increasing. Generally, trajectory optimization methods can be divided into two groups: direct methods and indirect methods (Betts, 1998). Indirect methods use Pontryagin's minimum principle to transform optimal control problem into a boundary-value problem. Indirect methods guarantee the optimality of the solution, while the boundary-value problem is hard to solve and sensitive to initial guess. In contrast, direct methods discretize the original optimal control problem into a parameter optimization problem and solve the parameter optimization problem by nonlinear programming (NLP) algorithms. With the development of NLP algorithms, large-scale NLP problems can be solved precisely. However, the solving process is rather time-consuming for complicated trajectory optimization problems. Consequently, traditional

approaches may be not suitable for onboard applications.

Recently, convex optimization has attracted wide attention due to its application in aerospace guidance and control, such as Mars powered landing (Acikmese et al., 2005; Acikmese et al., 2007; Blackmore et al., 2010), low-thrust orbit transfers (Wang and Grant, 2017¹), spacecraft rendezvous (Lu and Liu, 2013), path planning for unmanned aerial vehicles (Wang and Liu, 2017) and constrained missile guidance (Liu et al., 2016). Convex optimization can be divided into several subclasses, including linear programming (LP), quadratic programming (QP), second-order cone programming (SOCP), and semidefinite programming (SDP). If the optimization problem is formulated as one of them, it can be solved in polynomial time (Boyd et al., 2004). Mature primal-dual interior-point method (IPM) has been investigated to solve the convex optimization problem (Wright, 1997). With IPM, the globally optimal solution can be found in a number of iterations with deterministic upper bound. Besides, initial guesses are not required in IPM. With these advantages, convex optimization is a very promising approach for onboard trajectory optimization. However, highly nonlinear dynamics and constraints are the main difficulties for the application of convex

^a  <https://orcid.org/0000-0002-7583-7628>

^b  <https://orcid.org/0000-0003-2666-836X>

^c  <https://orcid.org/0000-0003-4224-9579>

^d  <https://orcid.org/0000-0003-0951-5126>

optimization. A SOCP method was developed for entry trajectory optimization problem where the dynamics equations with respect to the variable of energy were used (Liu et al., 2015¹). The original dynamics was relaxed into a SOCP form via successive linearization. On the base of this work, the smooth entry problem and maximum-crossrange entry problem were investigated using similar way (Liu et al., 2015²; Liu and Shen, 2016). Distinguish from (Liu et al., 2015¹), a sequential convex programming (SCP) algorithm was designed (Wang and Grant, 2017²), where the original dynamics with respect to time were used and the rate of bank angle was extended to a new control variable. Then this algorithm was used to design an autonomous entry guidance method (Wang and Grant, 2018).

The approaches mentioned above employ trapezoidal rule with uniform distributions of nodes as the discretization method, leading to low discretization precision (Sagliano, 2017). Moreover, only fixed-flight-time problem is considered, and the final flight time cannot be optimized, which is obviously not suitable for practical flight. Pseudospectral (PS) method, which discretizes the state and control variables on orthogonal collocation points, may be an alternative approach for entry trajectory optimization (Fahroo and Ross, 2008). The state and control variables are approximated by global Lagrange interpolations, resulting in higher discretization precision and smoother results. The total time domain is transformed to $[-1, 1]$, making PS method suitable for free-time problem. To solve powered landing problems, convex optimization has been combined with PS method. Acikmese et al. firstly used Chebyshev polynomials to interpolate the controls (Acikmese et al., 2005). Sagliano proposed the pseudospectral convex optimization for powered descent guidance with more precise results than standard convex methods (Sagliano, 2017; Sagliano, 2018). The pseudospectral sequential convex optimization is embedded into the model predictive control framework for rocket vertical landing guidance (Wang et al., 2019).

However, in standard PS method, the state variable on each node is associated with all state variables, since the Lagrange interpolation is a global interpolation method, leading to a less sparse structure of the underlying matrices. Thus the CPU time after discretization is quite longer than other methods, such as Euler method and trapezoidal rule. In this paper, the hp PS method and the sequential convex programming are united in one framework to alleviate this effect for the entry trajectory optimization problem. In hp PS method, which has

been implemented successfully in other optimization packages (Patterson and Rao, 2014), the whole time domain is broken into several subdomains and the state variable is only associated with the state variables of each subdomain. Therefore, compared with standard PS method, faster results with similar accuracy can be obtained.

This paper is organized as follows: In Section 2, the entry trajectory optimization problem is described. Section 3 presents the whole hp pseudospectral sequential convex programming (hp-PSCP) method. The numerical results are shown in Section 4 and the work is summarized in Section 5.

2 PROBLEM FORMULATION

In this section, we formulate the optimal control problem derived from the entry trajectory optimization problem.

2.1 Entry Dynamics

This paper considers Earth as a non-rotating spherical model. Instead of the energy-based equations for entry vehicles, we use the original equations of motion. The dimensionless three degree of freedom equations of motion of an entry vehicle are (Lu, 2014)

$$\begin{cases} \dot{r} = V \sin \theta \\ \dot{\lambda} = V \cos \theta \sin \psi / (r \cos \phi) \\ \dot{\phi} = V \cos \theta \cos \psi / r \\ \dot{V} = -D - \sin \theta / r^2 \\ \dot{\theta} = L \cos \sigma / V + (V^2 - 1 / r) \cos \theta / (Vr) \\ \dot{\psi} = L \sin \sigma / (V \cos \theta) + V^2 \cos \theta \sin \psi \tan \phi / r \end{cases} \quad (1)$$

where r is the dimensionless radius from the Earth center to the vehicle, which is normalized by $R_0 = 6371\text{km}$. λ and ϕ denotes the longitude and latitude, respectively. V denotes the dimensionless flight velocity, which is normalized by $\sqrt{g_0 R_0}$ with $g_0 = 9.81\text{m/s}^2$. θ denotes the flight path angle and ψ denotes the heading angle. σ is the bank angle. The dimensionless time t in the differentiation of the equations (1) is normalized by $\sqrt{R_0 / g_0}$. L and D denote the dimensionless lift and drag accelerations, respectively, which is normalized by g_0 .

$$\begin{cases} L = R_0 \rho V^2 C_L(\alpha, V) S_{ref} / (2m) \\ D = R_0 \rho V^2 C_D(\alpha, V) S_{ref} / (2m) \end{cases} \quad (2)$$

where m is the mass, S_{ref} is the reference area, C_L and C_D are the lift and drag coefficients, respectively, which are functions of angle of attack α and velocity, ρ is the atmospheric density calculated by

$$\rho(h) = \rho_0 e^{-h/h_0} \quad (3)$$

where h is the altitude, ρ_0 is the atmospheric density at sea level and h_0 is an altitude constant.

In this paper, the angle of attack α is assumed as a function of velocity. The bank angle σ is the only control variable for trajectory optimization. Furthermore, following the way in [16], we choose the bank angle rate, $\dot{\sigma}$, as the new control variable to constrain the change rate of bank angle and eliminate the potential high-frequency oscillations, that is,

$$\dot{\sigma} = u \quad (4)$$

where u is new control variable. By adding equations (4) to the original equations of motion (1), the augmented equations of motion can be transformed into an affine form:

$$\dot{\mathbf{x}} = \mathbf{f}(\mathbf{x}) + \mathbf{B}u \quad (5)$$

where $\mathbf{x} = [r; \lambda; \phi; V; \theta; \psi; \sigma]$ is state vector with seven elements. The function $\mathbf{f}(\mathbf{x})$ and matrix \mathbf{B} are given by

$$\mathbf{f}(\mathbf{x}) = \begin{bmatrix} V \sin \theta \\ V \cos \theta \sin \psi / (r \cos \phi) \\ V \cos \theta \cos \psi / r \\ -D - \sin \theta / r^2 \\ L \cos \sigma / V + (V^2 - 1/r) \cos \theta / (Vr) \\ L \sin \sigma / (V \cos \theta) + V^2 \cos \theta \sin \psi \tan \phi / r \\ 0 \end{bmatrix} \quad (6)$$

$$\mathbf{B} = [0; 0; 0; 0; 0; 0; 1] \quad (7)$$

In this new model, the control variable is decoupled from the states, which will potentially benefit the convergence of the follow-up hp-PSCP algorithms.

2.2 Trajectory Optimization Problem

For an entry flight, the initial and terminal state vectors are predefined:

$$\mathbf{x}(t_0) = \mathbf{x}_0, \quad \mathbf{x}(t_f) = \mathbf{x}_f \quad (8)$$

where \mathbf{x}_0 is the initial state and \mathbf{x}_f is the given terminal state. t_0 is the initial flight time and t_f is the free final flight time. During the entry flight, both the states and control are bounded:

$$\mathbf{x} \in [\mathbf{x}_{\min}, \mathbf{x}_{\max}] \quad (9)$$

$$|u| \leq u_{\max} \quad (10)$$

where u_{\max} is the upper bound of the bank angle rate, and $\mathbf{x}_{\min}, \mathbf{x}_{\max}$ are the lower and upper bounds of the states, respectively. Besides, the typical path constraints, including heat rate, dynamic pressure and normal load, are considered

$$\dot{Q} = k_Q \rho^{0.5} V^{3.15} \leq \dot{Q}_{\max} \quad (11)$$

$$q = \rho V^2 / 2 \leq q_{\max} \quad (12)$$

$$n = \sqrt{L^2 + D^2} \leq n_{\max} \quad (13)$$

where k_Q is a constant, and \dot{Q}, q, n are the heating rate, the dynamic pressure and the normal load, respectively. $\dot{Q}_{\max}, q_{\max}, n_{\max}$ are the upper bounds of them, respectively.

In this paper, a general cost function is considered as follows:

$$J = \varphi[\mathbf{x}(t_f)] + \int_{t_0}^{t_f} l(\mathbf{x}, \mathbf{u}) dt \quad (14)$$

Based on above discussion, the entry trajectory optimization can be defined as a nonlinear optimal control problem as follows:

Problem 0:

Minimize: (14)

Subject to: (5), (8)-(13)

P0 is a free-time optimal control problem, and the terminal flight time can be optimized (instead of fixed offline) which is a significant difference from (Liu et al., 2015¹; Wang and Grant, 2017²) and more accordant with practical flight.

3 TRAJECTORY OPTIMIZATION ALGORITHM

3.1 Flipped Radau Pseudospectral Method

For solving optimal control problem, numerical methods are usually divided into two classes: direct methods and indirect methods. In direct methods, the dynamics equations are discretized and the optimal control problem is transformed into a finite dimensional NLP problem. Among direct methods, pseudospectral (PS) methods discretize the state and control variables on orthogonal collocation points simultaneously. PS methods have high discretization precision and converge faster for smooth problems. Among a variety of PS methods, in this paper, we choose the flipped Radau pseudospectral method (FRPM). It has been proved that FRPM owns a smoother convergence with respect to other PS methods.

FRPM is an asymmetric PS method. First, we introduce the flipped Legendre-Gauss-Radau (LGR) polynomial

$$R_n(\tau) = L_n(\tau) - L_{n-1}(\tau) \quad \tau \in [-1, 1] \quad (15)$$

where $R_n(\tau)$ denotes the flipped Legendre-Gauss-Radau polynomial of order n and $L_n(\tau)$ denotes the Legendre polynomial of order n . n LGR points are the roots of $R_n(\tau)$ on $(-1, 1]$ and are chosen as the collocation nodes of FRPM. Besides, -1 is chosen as the first discretization node. Then there are $n+1$ discretization nodes on $[-1, 1]$ in FRPM.

In FRPM, the state and control variables are represented by orthogonal polynomials defined on $[-1, 1]$. The time domain of the optimal control problem is normalized by the affine transformation

$$\tau = \frac{2t}{t_f - t_0} - \frac{t_f + t_0}{t_f - t_0} \quad (16)$$

The state and control variables are approximated by Lagrange interpolations

$$\mathbf{x}(\tau) \cong \sum_{i=0}^n \mathbf{x}(\tau_i) P_i(\tau), \quad \mathbf{u}(\tau) \cong \sum_{i=1}^n \mathbf{u}(\tau_i) \bar{P}_i(\tau) \quad (17)$$

where $P_i(\tau)$ and $\bar{P}_i(\tau)$ are the Lagrange interpolation polynomials. Though Lagrange interpolation, the

derivative of $\mathbf{x}(\tau)$ can be approximated by the linear summation of $\mathbf{x}(\tau_i)$. Then the flipped Radau pseudospectral differentiation matrix \mathbf{D} is introduced (Patterson and Rao, 2014).

$$\frac{d\mathbf{x}(\tau_k)}{d\tau} = \sum_{i=0}^n \mathbf{D}_{ki} \mathbf{x}(\tau_i), \quad k = 1, \dots, n \quad (18)$$

At n LGR points, the dynamics equations are transformed into algebraic constraints by using (18)

$$\sum_{i=0}^n \mathbf{D}_{ki} \mathbf{x}(\tau_i) - \frac{t_f - t_0}{2} \mathbf{F}[\mathbf{x}(\tau_k), \mathbf{u}(\tau_k)] = 0, \quad k = 1, \dots, n \quad (19)$$

where $\mathbf{F}(\mathbf{x}, \mathbf{u})$ is the right-hand side of the dynamics equation.

Similarly, the cost function (14) can be replaced by

$$J = \varphi[\mathbf{x}(1)] + \frac{t_f - t_0}{2} \sum_{k=1}^n w_k l[\mathbf{x}(\tau_k), \mathbf{u}(\tau_k)] \quad (20)$$

where w_k is the corresponding weight at the LGR points.

3.2 hp Flipped Radau Pseudospectral Method

In the basic FRPM, which is introduced in the last section, the whole time domain $[t_0, t_f]$ is mapped against the pseudospectral time $[-1, 1]$. Thus, it is also called the global FRPM. With the increase of collocation nodes in this interval, the obtained solution becomes more accurate. It also means that the degree of the interpolation polynomials is increased to approximate the state and control variables, for example, by using p nodes. The global FRPM is called a p -method, since p is the only parameter that is used to control. However, in global FRPM, the state variable on each collocation node is associated with all state variables owing to the algebraic constraint (19), since the Lagrange interpolation is a global interpolation method. This characteristic leads to a less sparse structure of the underlying matrices, and the CPU time after discretization is much larger than common methods, such as Euler method and trapezoidal method.

On the other hand, we can break the whole time domain into a number of sub-domains, and the state variables are approximated by Lagrange interpolation locally on each sub-domain. In this way, the number

of segments h , and the number of nodes p for each segment, are the two parameters we define. This is the primary idea of so-called hp method, which has been introduced from computational fluid dynamics to discretization methods for optimal control (Patterson and Rao, 2014). Moreover, adaptive mesh refinements technology can be adopted to improve the discretization accuracy by updating the size of h and p . However, in this paper, we just use constant values of h and p , and the same number of nodes for each segment, for simplification. In hp FRPM, the state variable on each collocation node is only associated with the state variables of each segment, and the CPU time is significantly reduced.

In this paper we give the following notations: subscripts i denotes the i th node in a certain segment, and superscripts j define the j th segment, such as

$$\mathbf{x}_i^j, \mathbf{u}_i^j, \quad i = 1, \dots, p; \quad j = 1, \dots, h \quad (21)$$

$\mathbf{x}_i^j, \mathbf{u}_i^j$ represent the state and control variables at the i th node on the j th segment. Correspondingly, the time domain for each segment is defined as

$$[t_0^j, t_f^j], \quad j = 1, \dots, h \quad (22)$$

Then in the hp FRPM, the algebraic constraints (19) on the j th segment can be rewritten in the hp form:

$$\sum_{i=0}^p \mathbf{D}_{ki} \mathbf{x}_i^j - \frac{t_f - t_0}{2h} F[\mathbf{x}_i^j, \mathbf{u}_i^j] = 0, \quad k = 1, \dots, p \quad (23)$$

And the cost function is formulated as

$$J = \varphi[\mathbf{x}(\mathbf{x}_p^h)] + \frac{t_f - t_0}{2h} \sum_{j=1}^h \sum_{i=1}^p w_i l[\mathbf{x}_i^j, \mathbf{u}_i^j] \quad (24)$$

Moreover, the state variable on the last time node in the previous segment must equal to the one on the first time node in the latter segment, which is called the linking condition:

$$\begin{aligned} t_p^{j-1} &= t_0^j \\ \mathbf{x}_p^{j-1} &= \mathbf{x}_0^j, \quad j = 2, \dots, h \end{aligned} \quad (25)$$

3.3 hp Pseudospectral Sequential Convex Programming

With the hp FRPM, the dynamics equation (5) can be formulated as

$$\begin{aligned} 2h \sum_{i=0}^p \mathbf{D}_{ki} \mathbf{x}_i^j + \bar{\mathbf{f}}(\mathbf{x}_i^j) + \bar{\mathbf{B}}\mathbf{u} &= 0, \quad k = 1, \dots, p \\ \bar{\mathbf{f}}(\mathbf{x}_i^j) &= (t_0 - t_f) \mathbf{f}(\mathbf{x}_i^j) \\ \bar{\mathbf{B}} &= (t_0 - t_f) \mathbf{B} \end{aligned} \quad (26)$$

where t_f is a special control variable and t_0 is zero or other constant. Obviously, nonlinear terms exist in

$\bar{\mathbf{f}}(\mathbf{x}_i^j) + \bar{\mathbf{B}}\mathbf{u}$, while $2h \sum_{i=0}^p \mathbf{D}_{ki} \mathbf{x}_i^j$ is linear about state variables. Using first-order Taylor-series expansion, nonlinear terms can be linearized and become convex.

$$\begin{aligned} 2h \sum_{i=0}^p \mathbf{D}\mathbf{x}_i^j + (t_0 - t_f^k) \cdot \mathbf{f}(\mathbf{x}^k) + \mathbf{A}(\mathbf{x}^k, t_f^k) \cdot (\mathbf{x} - \mathbf{x}^k) + \\ \mathbf{T}(\mathbf{x}^k, t_f^k) \cdot (t_f - t_f^k) + (t_0 - t_f^k) \mathbf{B}\mathbf{u}^k + (t_0 - t_f^k) \mathbf{B} \cdot (\mathbf{u} - \mathbf{u}^k) \\ - \mathbf{B}\mathbf{u}^k \cdot (t_f - t_f^k) = 0 \end{aligned} \quad (27)$$

where the $(\mathbf{x}^k, \mathbf{u}^k, t_f^k)$ represents the reference trajectory and is the solution at k th iteration. $\mathbf{A} = \partial \bar{\mathbf{f}} / \partial \mathbf{x}$, $\mathbf{T} = \partial \bar{\mathbf{f}} / \partial t_f$. Rearranging equation (27) obtains

$$\begin{aligned} 2h \sum_{i=0}^p \mathbf{D}\mathbf{x}_i^j + \mathbf{A}(\mathbf{x}^k, t_f^k) \cdot \mathbf{x} + \mathbf{B}(t_0 - t_f^k) \cdot \mathbf{u} + \\ [\mathbf{T}(\mathbf{x}^k, t_f^k) - \mathbf{B}\mathbf{u}^k] \cdot t_f + \mathbf{W}(\mathbf{x}^k, \mathbf{u}^k, t_f^k) = 0 \\ \mathbf{W}(\mathbf{x}^k, \mathbf{u}^k, t_f^k) = (t_0 - t_f^k) \cdot \mathbf{f}(\mathbf{x}^k) + (t_0 - t_f^k) \mathbf{B}\mathbf{u}^k \\ - \mathbf{A}(\mathbf{x}^k, t_f^k) \mathbf{x}^k - \mathbf{T}(\mathbf{x}^k, t_f^k) \cdot t_f^k - (t_0 - t_f^k) \mathbf{B}\mathbf{u}^k + \mathbf{B}\mathbf{u}^k \cdot t_f^k \end{aligned} \quad (28)$$

Then equation (28) is linear and convex about state and control variables. A trust-region constraint is added to ensure the validity of linearization as follows

$$\|\mathbf{x} - \mathbf{x}^k\| \leq \delta \quad (29)$$

where δ is the constant radius of the trust region.

Note that path constraints (11-13) are the functions of r and V . First-order Taylor-series expansion is also used to linearize nonlinear path constraints.

$$\begin{aligned} f_{\dot{Q}}(r,V) &= f_{\dot{Q}}(r^k,V^k) + \frac{\partial f_{\dot{Q}}}{\partial r}(r-r^k) + \frac{\partial f_{\dot{Q}}}{\partial V}(V-V^k) \leq \dot{Q}_{\max} \\ f_q(r,V) &= f_q(r^k,V^k) + \frac{\partial f_q}{\partial r}(r-r^k) + \frac{\partial f_q}{\partial V}(V-V^k) \leq q_{\max} \quad (30) \\ f_n(r,V) &= f_n(r^k,V^k) + \frac{\partial f_n}{\partial r}(r-r^k) + \frac{\partial f_n}{\partial V}(V-V^k) \leq n_{\max} \end{aligned}$$

where $f_{\dot{Q}}(r,V)$, $f_q(r,V)$, $f_n(r,V)$ denote the heating rate, dynamic pressure and normal load constraints, respectively.

As for the cost function (14), in this paper, we choose the following form

$$J = \int_{t_0}^{t_f} (|\dot{h} - k_c| + k_1 \cdot |\dot{\sigma}|) dt \quad (31)$$

In this cost function, the first term is to make the descent rate of the vehicle close to a constant and smooth the trajectory. The second term is to avoid the high-frequency oscillations in bank angle. k_c is the desired descent rate and k_1 is the weight coefficient. Obviously, this cost function has a nonlinear integrand and must be linearized. Combing with the hp form (24), it becomes

$$J = \frac{1}{2h} \sum_{j=1}^h \sum_{i=1}^p w_i (|(t_f - t_0)(\dot{h} - k_c)| + k_1 \cdot |(t_f - t_0)u|) \quad (32)$$

Introducing two slack variables η_1, η_2 , the cost function is equivalently converted into

$$J = \frac{1}{2h} \sum_{j=1}^h \sum_{i=1}^p w_i (\eta_1 + k_1 \cdot \eta_2) \quad (33)$$

subjects to additional constraints

$$\begin{aligned} |f_{J_1}| &\leq \eta_1, \quad f_{J_1} = (t_f - t_0)(V \sin \theta - k_c) \\ |f_{J_2}| &\leq \eta_2, \quad f_{J_2} = (t_f - t_0)u \end{aligned} \quad (34)$$

Linearizing f_{J_1} and f_{J_2} around the reference trajectory gives

$$\begin{aligned} &|(t_f^k - t_0)(V^k \sin \theta^k - k_c) + \frac{\partial f_{J_1}}{\partial t_f}(t_f - t_f^k) \\ &+ \frac{\partial f_{J_1}}{\partial V}(V - V^k) + \frac{\partial f_{J_1}}{\partial \theta}(\theta - \theta^k)| \leq \eta_1 \\ &|(t_f^k - t_0)u^k + \frac{\partial f_{J_2}}{\partial t_f}(t_f - t_f^k) + \frac{\partial f_{J_2}}{\partial u}(u - u^k)| \leq \eta_2 \end{aligned} \quad (35)$$

Then cost function (33) is a linear function about η_1, η_2 subject to linear constraints (35). All the nonlinear constraints have been linearized.

Problem 1:

Minimize: (33)

Subject to: (8),(9),(10),(28),(29),(30),(35)

Assuming that the hp pseudospectral discretization is sufficiently precise and the real trajectory (\mathbf{x}, u, t_f) is close enough to the reference trajectory $(\mathbf{x}^k, u^k, t_f^k)$ so that the problem P1 is a good approximation of the original problem P0. In this paper, we solve problem 0 equivalently by solving a sequence of convex optimal control problems formulated by problem 1 using the solution from the previous iteration. The solution process is summarized as follows:

1) Set $k = 0$. Propagate the equations of motion (1) with initial conditions and a certain control profile to provide an initial trajectory $(\mathbf{x}^0, u^0, t_f^0)$ for the solution procedure.

2) At the k th iteration ($k \geq 1$), set up problem P1 by using $(\mathbf{x}^{k-1}, u^{k-1}, t_f^{k-1})$. Then, solve problem P1 to find the solution $(\mathbf{x}^k, u^k, t_f^k)$ by the primal-dual interior-point method.

3) Check whether the convergence condition is satisfied

$$\max_{t_0 \leq t \leq t_f} |\mathbf{x}^k - \mathbf{x}^{k-1}| \leq \boldsymbol{\varepsilon} \quad (36)$$

where $\boldsymbol{\varepsilon}$ is predefined tolerance vector for convergence. If this condition is satisfied, go to Step 4; otherwise set $k = k + 1$ and go back to Step 2.

4) The solution is found to be $(\mathbf{x}^k, u^k, t_f^k)$.

4 NUMERICAL RESULTS

In this section, numerical results are carried out to demonstrate the effectiveness of the algorithms proposed in this paper. The entry vehicle model adopted in the simulation is the CAV-H (Phillips, 2003). The mass of CAV-H is 907.2 kg and the reference area is 0.4939m². The path constraints and control constraints are set as follows:

$$\begin{aligned} \dot{Q}_{\max} &= 1200 \text{kw} / \text{m}^2, \quad q_{\max} = 150 \text{kpa}, \quad n_{\max} = 3 \\ -90^\circ &\leq \sigma \leq 90^\circ \end{aligned} \quad (37)$$

The angle of attack profile is designed as

$$\alpha = \begin{cases} 20^\circ & V \geq 6500 \text{m/s} \\ \frac{9^\circ}{1500}(V - 5000) + 11^\circ & 5000 \text{m/s} \leq V < 6500 \text{m/s} \\ 11^\circ & V < 5000 \text{m/s} \end{cases} \quad (38)$$

The entry mission is set as

Table 1: Entry mission.

States	$h(\text{km})$	λ (°)	ϕ (°)	$V(\text{m/s})$	θ (°)	ψ (°)
x_0	80	10	-20	7100	-1	45
x_f	30	90	30	2500	-	-

To give convincing results, we solve the optimization problem with three methods, respectively. The first method is the standard sequential convex programming (SCP), which uses the trapezoidal discretization (Wang and Grant, 2017²). The second method is the pseudospectral sequential convex programming (PSCP), which use the Flipped Radau pseudospectral discretization (Wang et al., 2019). The third method is the proposed hp-PSCP. In these three methods, the total number of discretization nodes is set to 201. Especially, in hp-PSCP, $h=10$ and $p=20$. The radius of the trust region is given as

$$\delta = \left[\frac{5000}{R}, \frac{5\pi}{180}, \frac{5\pi}{180}, \frac{500}{V_0}, \frac{5\pi}{180}, \frac{5\pi}{180}, \frac{10\pi}{180} \right]^T \quad (39)$$

The convergence condition is given as

$$\varepsilon = \left[\frac{200}{R}, \frac{0.1\pi}{180}, \frac{0.1\pi}{180}, \frac{1}{V_0}, \frac{0.1\pi}{180}, \frac{0.1\pi}{180}, \frac{1\pi}{180} \right]^T \quad (40)$$

The optimization problems are modeled using YALMIP (Lofberg, 2004), and are solved by MOSEK (Andersen et al., 2003). All the simulations are performed in MATLAB 2016a on a PC with an Intel Core i5.

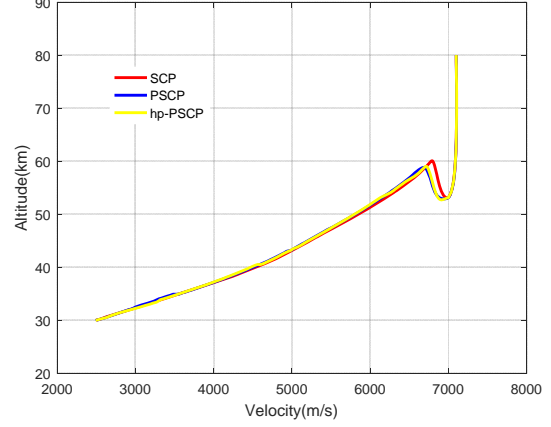


Figure 1: The altitude-velocity profiles in three methods.

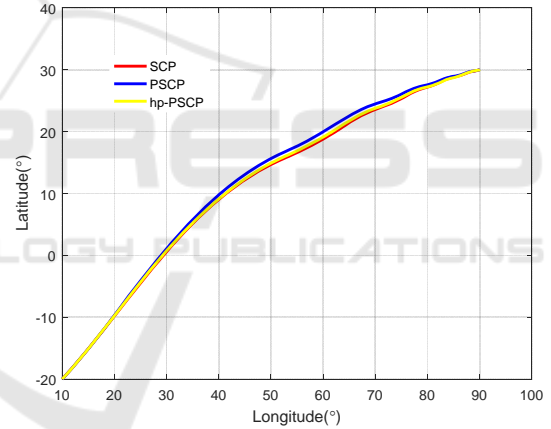


Figure 2: The ground tracks in three methods.

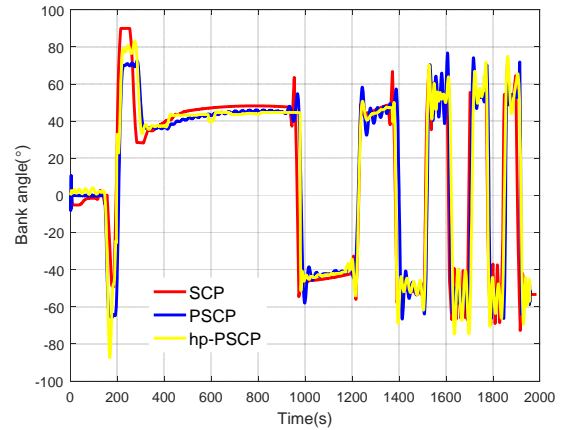


Figure 3: The bank angle profiles in three methods.

The solutions in three methods are shown in Fig.1-3. The altitude-velocity profiles and ground tracks basically coincide. The entry trajectory is very smooth. The bank angle profiles have similar trend with slight difference, which may result from different discretization methods.

To verify the accuracy of the solutions, we compare the optimal trajectories and trajectories obtained by propagating the dynamics equations (1) with optimal controls in three methods. The classical Runge-Kutta method is used and the terminal condition of propagation is reaching the terminal velocity. The propagated and optimal trajectories are displayed in Fig.4-6. The errors between the optimal terminal states and the propagated terminal states are given in Tab.2. As we can see, in the Fig.4-6, the propagated trajectory does not coincide with the optimal trajectory in SCP, while the propagated and optimal trajectories match well in PSCP and hp-PSCP. In Tab.2, the terminal errors of SCP, especially the terminal longitude and latitude errors are quite large, which is unacceptable even though the CPU time is the shortest. As for PSCP, the terminal accuracy is very high. However, the CPU time is one order higher than the other two methods. By contrast, the proposed hp-PSCP reduces the terminal errors significantly with respect to SCP with little growth of CPU times. In other words, the hp-PSCP method achieves a good trade-off between computational accuracy and speed.

Table 2: Comparison of Terminal errors and CPU times for each iteration.

States	$e_h(m)$	$e_\lambda(^{\circ})$	$e_\phi(^{\circ})$	$e_v(m)$	CPU time
SCP	-61.6	1.61	0.61	-1.34	0.12
PSCP	20.3	-0.007	0.01	-1.42	2.45
Hp-PSCP	25.3	-0.04	0.05	-1.71	0.21

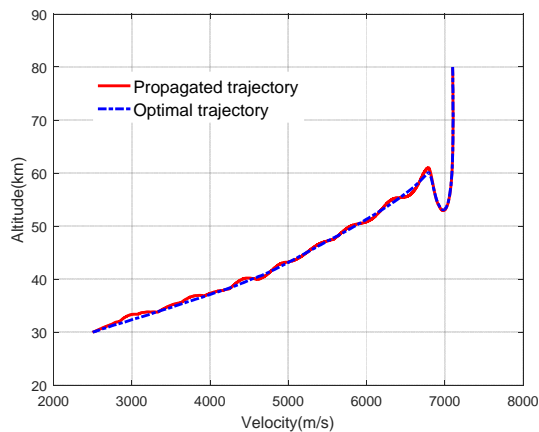


Figure 4: The propagated and optimal trajectories in SCP.

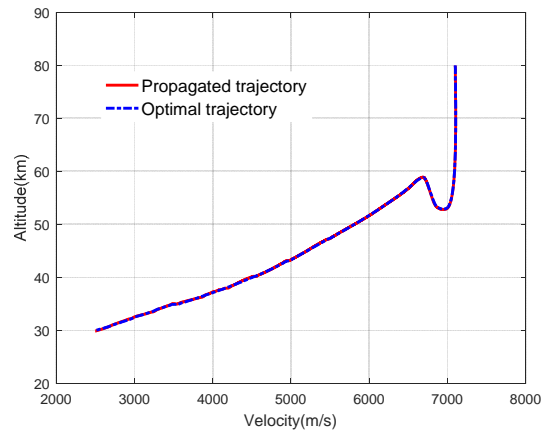


Figure 5: The propagated and optimal trajectories in PSCP.

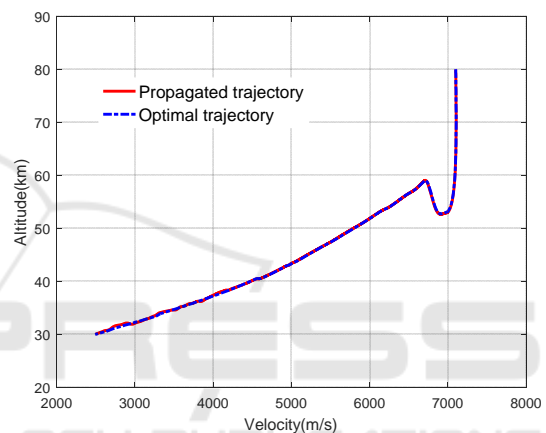


Figure 6: The propagated and optimal trajectories in hp-PSCP.

5 CONCLUSION

In this paper, the hp pseudospectral method and sequential convex programming are combined to solve the entry trajectory optimization problem. The hp flipped Radau pseudospectral method is employed to get more accurate results without much larger computational cost compared to standard convex approaches. Numerical results confirm that the proposed method results in a significant decline of computation time with limited impact on solution accuracy with respect to pseudospectral convex programming. Future work includes the intensive study of the influence of h and p on solution results, and we will apply hp-PSCP to onboard guidance.

ACKNOWLEDGMENT

This work is supported by the National Natural Science Foundation of China (No. 11572036).

REFERENCES

- Andersen, E. D., Roos, C., & Terlaky, T. (2003). On implementing a primal-dual interior-point method for conic quadratic optimization. *Mathematical Programming*, 95(2), 249-277.
- Acikmese, B., & Ploen, S. R. (2005). A powered descent guidance algorithm for Mars pinpoint landing. In *AIAA Guidance, Navigation, and Control Conference and Exhibit* (p. 6288).
- Acikmese, B., & Ploen, S. R. (2007). Convex programming approach to powered descent guidance for mars landing. *Journal of Guidance, Control, and Dynamics*, 30(5), 1353-1366.
- Betts, J. T. (1998). Survey of numerical methods for trajectory optimization. *Journal of guidance, control, and dynamics*, 21(2), 193-207.
- Boyd, S., & Vandenberghe, L. (2004). *Convex optimization*. Cambridge university press.
- Blackmore, L., Acikmese, B., & Scharf, D. P. (2010). Minimum-landing-error powered-descent guidance for Mars landing using convex optimization. *Journal of guidance, control, and dynamics*, 33(4), 1161-1171.
- Fahroo, F., & Ross, I. M. (2008, August). Advances in pseudospectral methods for optimal control. In *AIAA guidance, navigation and control conference and exhibit* (p. 7309).
- Lu, P., & Liu, X. (2013). Autonomous trajectory planning for rendezvous and proximity operations by conic optimization. *Journal of Guidance, Control, and Dynamics*, 36(2), 375-389.
- Lu, P. (2014). Entry guidance: a unified method. *Journal of Guidance, Control, and Dynamics*, 37(3), 713-728.
- Liu, X., Shen, Z., & Lu, P. (2015). Entry trajectory optimization by second-order cone programming. *Journal of Guidance, Control, and Dynamics*, 39(2), 227-241.
- Liu, X., Shen, Z., & Lu, P. (2015). Solving the maximum-crossrange problem via successive second-order cone programming with a line search. *Aerospace Science and Technology*, 47, 10-20.
- Liu, X., Shen, Z., & Lu, P. (2016). Exact convex relaxation for optimal flight of aerodynamically controlled missiles. *IEEE Transactions on Aerospace and Electronic Systems*, 52(4), 1881-1892.
- Liu, X., & Shen, Z. (2016). Rapid smooth entry trajectory planning for high lift/drag hypersonic glide vehicles. *Journal of Optimization Theory and Applications*, 168(3), 917-943.
- Lofberg, J. (2004). YALMIP: A toolbox for modeling and optimization in MATLAB. In *Proceedings of the CACSD Conference* (Vol. 3).
- Patterson, M. A., & Rao, A. V. (2014). GPOPS-II: A MATLAB software for solving multiple-phase optimal control problems using hp-adaptive Gaussian quadrature collocation methods and sparse nonlinear programming. *ACM Transactions on Mathematical Software (TOMS)*, 41(1), 1.
- Phillips, T. H. (2003). A common aero vehicle (CAV) model, description, and employment guide. *Schafer Corporation for AFRL and AFSPC*, 27.
- Sagliano, M. (2017). Pseudospectral convex optimization for powered descent and landing. *Journal of Guidance, Control, and Dynamics*, 41(2), 320-334.
- Sagliano, M. (2018). Generalized hp Pseudospectral Convex Programming for Powered Descent and Landing. In *2018 AIAA Guidance, Navigation, and Control Conference* (p. 1870).
- Wright, S. J. (1997). *Primal-dual interior-point methods* (Vol. 54). Siam
- Wang, Z., Liu, L., & Long, T. (2017). Minimum-Time Trajectory Planning for Multi-Unmanned-Aerial-Vehicle Cooperation Using Sequential Convex Programming. *Journal of Guidance, Control, and Dynamics*, 40(11), 2976-2982.
- Wang, Z., & Grant, M. J. (2017). Optimization of Minimum-Time Low-Thrust Transfers Using Convex Programming. *Journal of Spacecraft and Rockets*, 55(3), 586-598.
- Wang, Z., & Grant, M. J. (2017). Constrained trajectory optimization for planetary entry via sequential convex programming. *Journal of Guidance, Control, and Dynamics*, 1-13.
- Wang, Z., & Grant, M. J. (2018). Autonomous entry guidance for hypersonic vehicles by convex optimization. *Journal of Spacecraft and Rockets*, 55(4), 993-1006.
- Wang, J., Cui, N., & Wei, C. (2019). Optimal Rocket Landing Guidance Using Convex Optimization and Model Predictive Control. *Journal of Guidance, Control, and Dynamics*, 1-15.